



## Rapid communication

Influence of sputtering atmosphere on the structural and magnetic properties of  $(\text{Bi}_{1-x}\text{Nd}_x)\text{FeO}_3$  thin films

Y.G. Wang, X.G. Tang\*, D.G. Chen, Q.X. Liu, Y.P. Jiang, D.P. Xiong

School of Physics &amp; Optoelectric Engineering, Guangdong University of Technology, Guangzhou Higher Education Mega Centre, Guangzhou 510006, People's Republic of China

## ARTICLE INFO

## Article history:

Received 8 March 2014

Accepted 11 April 2014

## Keywords:

BiFeO<sub>3</sub>

Thin film

Magnetron sputtering

Preferred growth

Magnetic property

## ABSTRACT

$(\text{Bi}_{1-x}\text{Nd}_x)\text{FeO}_3$  (BNF,  $x = 0.075$  and  $0.125$ ) thin films were grown on Si(100) substrates by radio frequency magnetron sputtering with various deposition atmospheres. It was found that the sputtering atmosphere has affected the phase structure, surface morphology and magnetic properties of BNF thin films. X-ray diffraction revealed that the BNF thin films exhibit highly (012)-orientation crystallization when the sputtering atmosphere is nitrogen ( $\text{N}_2$ ), while, the inter-phase  $\text{Bi}_2\text{O}_3$  was observed when the sputtering atmosphere is the mixture of argon and oxygen ( $\text{Ar}/\text{O}_2$ ). Compared with the thin film deposited in  $\text{Ar}/\text{O}_2$ , the films sputtered in  $\text{N}_2$  showed a smoother surface and significantly enhanced ferromagnetism. It was also found that the crystallization and ferromagnetic properties of the BNF thin films were enhanced when  $x$  is increased from 0.075 to 0.125. The observed macroscopic magnetization was concluded to be the result of suppressed space-modulated spin structure of BNF thin films.

© 2014 Elsevier Ltd. All rights reserved.

Multiferroic materials, with the coexistence of spontaneous magnetization and spontaneous polarization, have been of great interest due to their potential applications in spintronic devices, functional sensors and actuators [1]. Unfortunately, since the unique electron configurations required, single phase multiferroics materials are rare in nature [2]. BiFeO<sub>3</sub> with a rhombohedrally distorted perovskite structure is one of the best candidates characterized by the high ferroelectric Curie temperature ( $T_C \sim 1100$  K) and antiferromagnetic Néel temperature ( $T_N \sim 643$  K) [3]. Its spontaneous polarization originates from the stereochemical activity of the Bi lone electron pair, which will hybridize with both the empty  $6p^0$  orbitals of  $\text{Bi}^{3+}$  ion and the  $2p^6$  electrons of  $\text{O}^{2-}$  ion to form Bi–O covalent bonds, introducing off centering in the structure and hence ferroelectric order [4,5]. The G-type canted antiferromagnetic order in BiFeO<sub>3</sub> is mainly attributed to the Jahn–Teller structural distortion controlled by the partially filled  $3d$  orbitals of the  $\text{Fe}^{3+}$ , and follows a cycloidal spiral along the (110)-direction with a period of  $\sim 620$  Å [6,7]. As a result, the possible remnant magnetization permitted by the G-type canted antiferromagnetic order is canceled by the

incommensurately space-modulated spin structure, significantly restricting the release of weak ferromagnetism and potential magnetoelectric effect [8].

Efforts to release macroscopic magnetization in pure BiFeO<sub>3</sub> have focused largely on rare earth substitution in the Bi sublattice. It has been reported that rare earth (e.g., La, Nd, Gd, Sm or Dy) cations substitution for  $\text{Bi}^{3+}$  can effectively modulate the crystal structure parameters of BiFeO<sub>3</sub>, destroy the space-modulated spin structure, and realize the macroscopic ferromagnetism [9–13]. Among these, enhanced ferromagnetism and ferroelectricity in the  $(\text{Bi}_{1-x}\text{Nd}_x)\text{FeO}_3$  (BNF) have been reported by previous literatures [14–16], and the simultaneous piezoelectricity was also realized [17]. Besides, the improvement of large ferroelectric coercivity [18] and the leakage current density in the BNF [19], which have been largely impeding the multiferroic applications of BiFeO<sub>3</sub>, promote us to do more research on the BNF thin films. In the previous literature, much effort has been made to discuss the magnetic properties of BNF thin films deposited by chemical solution deposition [14,19] and pulsed laser deposition method [16,18], but the effect of deposition condition on the structure and magnetic properties of magnetron sputtering-derived BNF thin film has not been reported. It is known that the working atmosphere has influence on the structure and magnetic properties of Fe-doping or Mn-doping ZnO diluted magnetic semiconductor thin films

\* Corresponding author. Fax: +86 20 3932 2265.

E-mail address: [xgtang@gdut.edu.cn](mailto:xgtang@gdut.edu.cn) (X.G. Tang).

[20,21], respectively. Thus, in this work, we prepared single-phase  $(\text{Bi}_{1-x}\text{Nd}_x)\text{FeO}_3$  thin films by a radio frequency magnetron sputtering with various deposition atmospheres, and report the effect of deposition atmospheres on the structure and magnetic properties of  $(\text{Bi}_{1-x}\text{Nd}_x)\text{FeO}_3$  thin films.

The  $(\text{Bi}_{1-x}\text{Nd}_x)\text{FeO}_3$  ( $x = 0.075$  and  $0.125$ , respectively abbreviated as BNF7.5 and BNF12.5) thin films were grown on Si(100) substrate using radio frequency (RF) magnetron sputtering with ceramic targets of BNF7.5 and BNF12.5. These ceramics prepared details were described elsewhere [22]. During the sputtering process, the substrate temperature was kept at  $550^\circ\text{C}$ , and the depositing atmosphere is  $\text{Ar}/\text{O}_2$  (pressure ratio is 9:1) and  $\text{N}_2$ , respectively. The samples were then annealed at  $650^\circ\text{C}$  by a rapid thermal annealing furnace under oxygen atmosphere for 5 min. Details of the deposition conditions are given in Table 1. The Samples 1 and 2 are the BNF7.5 thin films deposited in  $\text{Ar}/\text{O}_2$  and  $\text{N}_2$  atmospheres, respectively. And the Sample 3 is the BNF12.5 thin film deposited in  $\text{N}_2$  atmospheres.

The thickness of the as-grown thin films on Si(100) substrates was measured by a surface profiler (KLA-Tencor P-10), which was about 200 nm. The crystalline structure of the BNF thin films was characterized at room temperature by X-ray diffraction (XRD, Rigaku D-MAX 2200) with  $\text{CuK}\alpha$  radiation. The surface morphology of the sample was investigated by atomic force microscopy (BenYuan, CSPM5500). And the magnetic properties of the films were measured using a vibrating sample magnetometer (VSM, Quantum Design, PPMS-9) at room temperature.

Fig. 1 shows the XRD patterns of the BNF thin films on Si(100) substrates. When the sputtering atmosphere is  $\text{Ar}/\text{O}_2$ , a poor crystallization and inter-phase  $\text{Bi}_2\text{O}_3$  was observed in sample 1. Reversely, when the sputtering atmosphere is  $\text{N}_2$ , the BNF thin films (sample 2 and 3) appear to be well crystallized at  $650^\circ\text{C}$ , and no secondary phases were detected, showing a pure rhombohedral (R3c) distorted perovskite structure [17,23]. There are three peaks, i.e. (012), (104) and (024), are observed in the sample 2 patterns and the intensity of (012) peak is much stronger than that of (104) one. The relative peak intensity of  $I(012)/[I(012) + I(104) + I(024)]$  is calculated to be 0.92, suggesting highly (012)-orientation growth for the BNF film on Si(100) substrate. The sample 3 (with more Nd ions) exhibits a more highly (012)-orientation growth with no (104) peak and good crystallization as well. The slight shift of the peak position (in sample 2 and 3) corresponds to the change of the lattice parameter, which was caused by the different concentrations of Nd substitution. The phase variation is consistent with the previous study, where single-phase  $\text{BiFeO}_3$  films can only be obtained in a rather narrow range of oxygen pressure and higher pressure will result in the  $\text{Bi}_2\text{O}_3$  precipitates [24].

The surface morphology of the BNF thin film was displayed in the Fig. 2. As we see, all samples exhibit a uniform microstructure

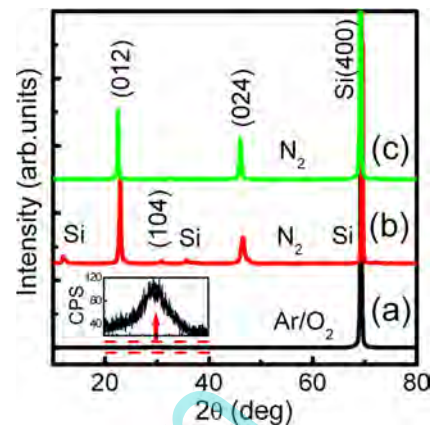


Fig. 1. X-ray diffraction patterns of the BNF thin films: (a) and (b) for BNF7.5 thin films deposited in  $\text{Ar}/\text{O}_2$  and  $\text{N}_2$  atmosphere, respectively; (c) for BNF12.5 thin film deposited in  $\text{N}_2$  atmosphere.

with no cracks. When deposited in the  $\text{Ar}/\text{O}_2$  atmosphere, the BNF7.5 thin film (sample 1) formed a relatively rough surface composed of cylindrical filaments, and the root mean square roughness (RMS) is 25.2 nm. However,  $\text{N}_2$  depositing has significantly reduced the surface roughness, and resulted in the relatively smooth and dense surface. The RMS of the BNF7.5 thin film deposited in  $\text{N}_2$  (sample 2) is 1.4 nm, which is much smaller than that of sample 1. Combined with the XRD results, the large RMS of the sample 1 is consistent with the poor crystallization, and the cylindrical filaments may be caused by the  $\text{Bi}_2\text{O}_3$  grains or the amorphous BNF. Besides, the RMS of the thin film was further reduced with increasing Nd-doping, that is, a smoother and denser surface with the RMS of 1.2 nm was obtained in the BNF12.5 thin film (sample 3).

Fig. 3 shows the magnetic hysteresis ( $M-H$ ) loops of the BNF thin films measured at room temperature by applying an in-plane magnetic field, and the central region of the hysteresis loop obtained for BNF12.5 thin film was magnified and shown in the inset. It is found that the weak ferromagnetism has been obtained through Nd substitution in all the thin films, with a small but nonzero remnant magnetization. The BNF thin films deposited in  $\text{N}_2$  atmosphere showed a better ferromagnetic property than the film deposited in the  $\text{Ar}/\text{O}_2$ . And the magnetization of the  $(\text{Bi}_{1-x}\text{Nd}_x)\text{FeO}_3$  thin films exhibits a large rise when  $x$  is increased from 0.075 to 0.125. The largest magnetic moment was obtained in the BNF12.5 thin film with the saturated magnetization, remnant magnetization, and coercivity of  $10.44 \text{ emu}/\text{cm}^3$ ,  $0.70 \text{ emu}/\text{cm}^3$  and  $84.40 \text{ Oe}$ , respectively.

Combined with the XRD and AFM results, the magnetic difference between the sample 1 and sample 2 may be caused by the various phase structure, and the difference between the well crystallized sample 2 and sample 3 needs our further discussion. There are mainly two possible causes that may account for the spontaneous magnetization of the BNF thin films: one is the possible existence of  $\text{Fe}^{2+}$  [18,25,26], and the other is the canting of the antiferromagnetically ordered spin induced by the lattice distortion [10,16]. It was reported that when introducing the  $\text{Fe}^{2+}$  with an out shell electron configuration of  $3d^6$  into  $\text{Fe}^{3+}$  with an out shell electron configuration of  $3d^5$ , the magnetic structure may be modified from antiferromagnetic to antiferromagnetic at the  $\text{Fe}^{2+}$  site [16]. However, due to the enhanced structural stability induced by Nd substitution, the content of  $\text{Fe}^{2+}$  is supposed to decrease with the increase of  $x$  [14], and the magnetization of the thin film will also reduce with the increasing  $x$ , which is

Table 1

Deposition conditions of BNF thin films by RF-magnetron sputtering method.

Deposition parameters	Sample nos.		
	1	2	3
Ceramic targets	$(\text{Bi}_{0.925}\text{Nd}_{0.075})\text{FeO}_3$		$(\text{Bi}_{0.875}\text{Nd}_{0.125})\text{FeO}_3$
Deposition temperature ( $^\circ\text{C}$ )	550	550	550
Films thickness (nm)	200	200	200
Base vacuum (Pa)	$2.67 \times 10^{-4}$	$2.67 \times 10^{-4}$	$2.67 \times 10^{-4}$
Sputtering power (W)	40	40	40
Deposition time (min)	300	300	300
Working pressure (Pa)	2.7	3.0	3.0
Sputtering atmosphere	$\text{Ar}/\text{O}_2$ (9/1)	$\text{N}_2$	$\text{N}_2$
Annealing temperature ( $^\circ\text{C}$ )	650	650	650

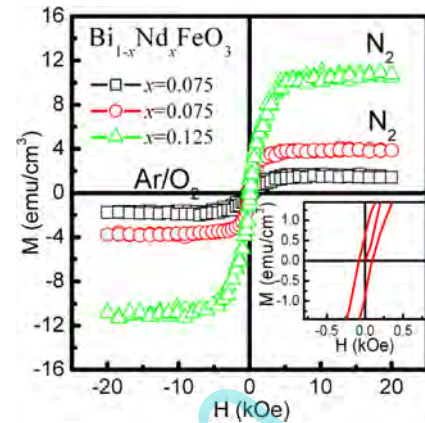
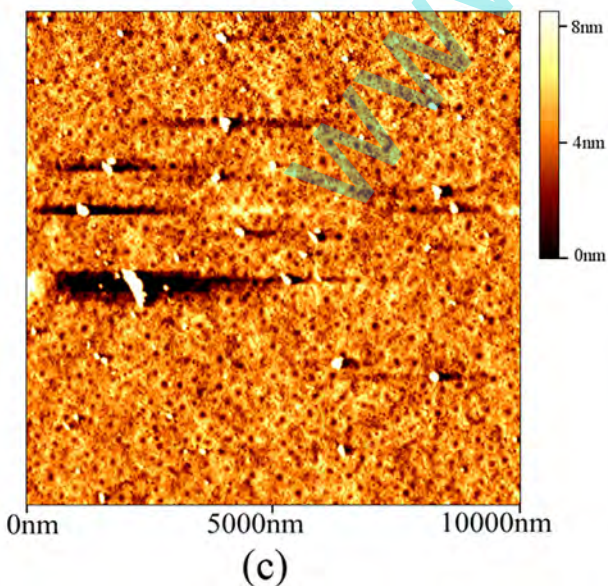
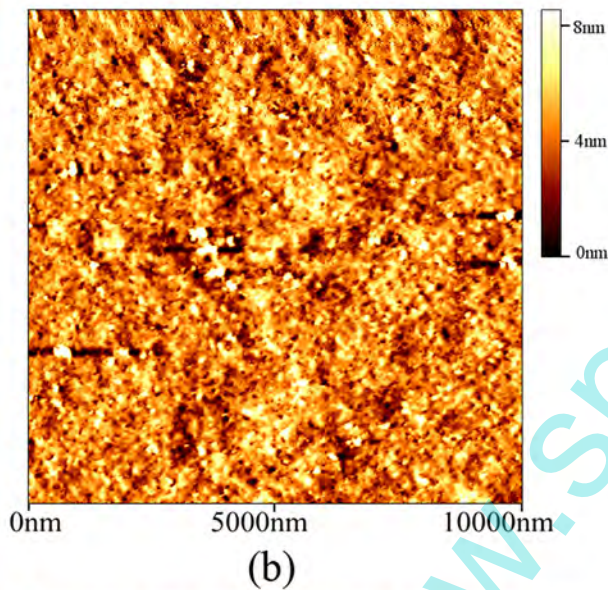
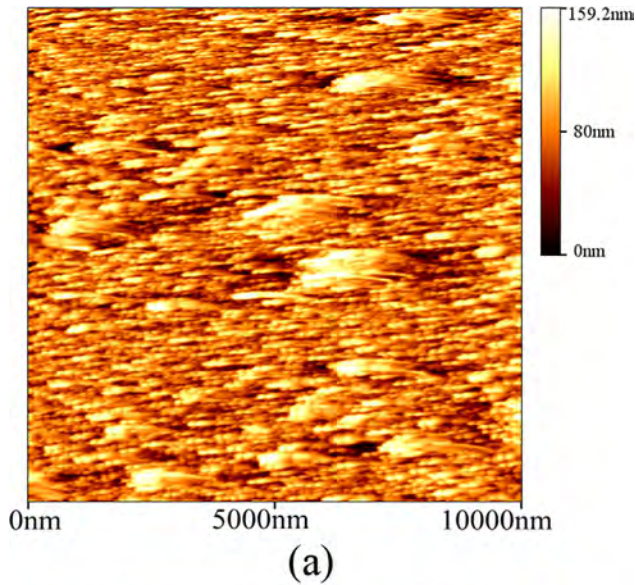


**Fig. 3.** Magnetic hysteresis loops ( $M-H$ ) of the BNF thin films. Inset represents the magnified view of the central region of the hysteresis loop obtained for BNF12.5 thin film.

obviously inconsistent with our experimental results. Therefore, the increased macroscopic magnetization in the sample 3 is likely due to the suppressed space-modulated spin structure induced by the Nd doping [15]. Nd dopant can result in a structural distortion in  $\text{BiFeO}_3$  thin films, which can suppress the inhomogeneous space-modulated spin structure, and release the latent magnetization locked within the antiferromagnetic order [13]. The explanation is quite consistent with our XRD and VSM results. The spontaneous moment in sample 1 could be attributed to the presence of ordered clusters in the amorphous film [27]. It has been reported that, after high temperature annealing, though the film exhibits an amorphous state macroscopically, there may still be some small crystalline grains wrapped in it [27]. This may also explain why there are so many cylindrical filaments on the surface of amorphous thin film. However, since the discussions above are just based on the straight-forward phenomenon, further studies are required to understand the magnetic behavior of BNF thin film. The low coercive magnetic fields of BNF thin films indicate that the thin films are suitable for use in devices.

In summary, Ferromagnetic  $(\text{Bi}_{1-x}\text{Nd}_x)\text{FeO}_3$  (BNF,  $x = 0.075$  and  $0.125$ ) thin films are deposited on  $\text{Si}(100)$  substrates by radio frequency magnetron sputtering with various deposition atmospheres. The deposition atmosphere was found to affect the phase structure, surface morphology, and magnetic properties of BNF thin films. X-ray diffraction measurement shows that the BNF exhibits highly (012)-orientation when the sputtering atmosphere is  $\text{N}_2$ , while, the inter-phase  $\text{Bi}_2\text{O}_3$  was observed when the sputtering atmosphere is  $\text{Ar}/\text{O}_2$ . The BNF thin films deposited in the  $\text{N}_2$  atmosphere showed a better crystallization, smoother surface and significantly enhanced ferromagnetism than the film deposited in the  $\text{Ar}/\text{O}_2$ . Besides, the magnetization of the  $(\text{Bi}_{1-x}\text{Nd}_x)\text{FeO}_3$  thin films exhibits a large rise when  $x$  is increased from  $0.075$  to  $0.125$ , with the saturated magnetization, remnant magnetization, and coercivity of  $10.44 \text{ emu}/\text{cm}^3$ ,  $0.70 \text{ emu}/\text{cm}^3$  and  $84.40 \text{ Oe}$ , respectively. The observed macroscopic magnetization in our samples is likely due to the suppressed space-modulated spin structure of BNF thin films.

**Fig. 2.** AFM micrographs of the surface morphology for BNF thin films: (a) and (b) for BNF7.5 thin films deposited in  $\text{Ar}/\text{O}_2$  and  $\text{N}_2$  atmosphere, respectively; (c) for BNF12.5 thin film deposited in  $\text{N}_2$  atmosphere.

## Acknowledgments

This work was supported by the National Natural Science Foundation of China (Grant Nos. 11032010, and 11202054), the Guangdong Provincial Natural Science Foundation of China (Grant Nos. 8151009001000003 and 10151009001000050), and the Guangdong Provincial Educational Commission of China (Grant No. 2012KJ CX0044).

## References

- [1] Eerenstein W, Mathur ND, Scott JF. *Nature* 2006;442:759–65.
- [2] Hill NA. *J Phys Chem B* 2000;104:6694–709.
- [3] Martin LW. *Dalt Trans* 2010;39:10813–26.
- [4] Fiebig M. *J Phys D Appl Phys* 2005;38:R123–52.
- [5] Seshadri R, Hill NA. *Chem Mater* 2001;13:2892–9.
- [6] Sosnowska I, Neumaier TP, Steichele E. *J Phys C Solid State Phys* 1982;15:4835–46.
- [7] Sosnowska I, Zvezdin AK. *J Magn Magn Mater* 1995;140–144:167–8.
- [8] Wang J, Neaton JB, Zheng H, Nagarajan V, Ogale SB, Liu B, et al. *Science* 2003;299:1719–22.
- [9] Zhang YJ, Zhang HG, Yin JH, Zhang HW, Chen JL, Wang WQ, et al. *J Magn Magn Mater* 2010;322:2251–5.
- [10] Khomchenko VA, Shvartsman VV, Borisov P, Kleemann W, Kiselev DA, Bdiikin IK, et al. *Acta Mater* 2009;57:5137–45.
- [11] Sosnowska I, Przenioso R, Fischer P, Murashov VA. *J Magn Magn Mater* 1996;160:384–5.
- [12] Nalwa KS, Garg A, Upadhyaya A. *Mater Lett* 2008;62:878–81.
- [13] Xu JM, Wang GM, Wang HX, Ding DF, He Y. *Mater Lett* 2009;63:855–7.
- [14] Huang FZ, Lu XM, Lin WW, Wu XM, Kan Y, Zhu JS. *Appl Phys Lett* 2006;89:242914.
- [15] Yuan GL, Or Siu Wing, Liu JM, Liu ZG. *Appl Phys Lett* 2006;89:052905.
- [16] Cheng ZX, Wang XL, Dou SX, Kimura H, Ozawa K. *J Appl Phys* 2008;104:116109.
- [17] Schiemer J, Withers RL, Carpenter MA, Liu Y, Wang JL, Norén L, et al. *J Phys Condens Matter* 2012;24:125901.
- [18] Yuan GL, Or Siu Wing, Chan HLW, Liu ZG. *J Appl Phys* 2007;101:024106.
- [19] Simões AZ, Cavalcante LS, Moura F, Longo E, Varela JA. *J Alloys Compd* 2011;509:5326–35.
- [20] Mera J, Córdoba C, Doria J, Paucar C, Gómez A, Fuchs D, et al. *Vacuum* 2012;86:1605–12.
- [21] Chen GJ, Tsai YY, Chang YS. *Vacuum* 2013;87:213–7.
- [22] Chen DG, Tang XG, Liu QX, Cheng XF, Zou Y. *Mater Sci Forum* 2011;687:439–46.
- [23] Tyholdt F, Fjellvåg H, Gunnæs AE, Olsen A. *J Appl Phys* 2007;102:074108.
- [24] Béa H, Bibes M, Barthélémy A, Bouzehouane K, Jacquet E, Khodan A, et al. *Appl Phys Lett* 2005;87:072508.
- [25] Tong JJ, Liu QX, Jiang YP, Tang XG, Zhou YC, Chen J. *Vacuum* 2011;86:340–3.
- [26] Béa H, Bibes M, Fusil S, Bouzehouane K, Jacquet E, Rode K, et al. *Phys Rev B* 2006;74:020101(R).
- [27] Chen J, Cheney S, Srinivasan G. *J Appl Phys* 1994;75:6828.